European Radiology (2021) 31:6275–6285
https://doi.org/10.1007/s00330-021-07710-6

CHEST

Vascular Ehlers–Danlos syndrome (vEDS): CT and histologic findings of pleural and lung parenchymal damage

Samia Boussouar[1] · Amira Benattia[2] · Jean.-Baptiste Escudié[3] · Laure Gibault[4] · Frédérique Capron[5] · Anne Legrand[6] · Pierre-Yves Brillet[7] · Xavier Jeunemaitre[6,8] · Philippe A. Grenier[9] · Elie Mousseaux[8,10] · Michael Frank[6,8] · Olivier Sanchez[11]

Received: 19 July 2020 / Revised: 17 December 2020 / Accepted: 21 January 2021 / Published online: 2 March 2021

Abstract

Objectives To describe CT features of lung involvement in patients with vascular Ehlers–Danlos syndrome (vEDS), a rare genetic condition caused by pathogenic variants within the *COL3A1* gene, characterized by recurrent arterial, digestive, and pulmonary events.

Material and methods All consecutive vEDS patients referred to the national tertiary referral center for vEDS, between 2004 and 2016, were included. Chest CT scans obtained during the initial vascular work-up were reviewed retrospectively by two chest radiologists for lung involvement. Five surgical samples underwent histologic examination.

Results Among 136 enrolled patients (83 women, 53 men; mean age 37 years) with molecularly confirmed vEDS, 24 (17.6%) had a history of respiratory events: 17 with pneumothorax, 4 with hemothorax, and 3 with hemoptysis that required thoracic surgery in 11. CT scans detected lung parenchymal abnormalities in 78 (57.3%) patients: emphysema (mostly centrilobular and paraseptal) in 44 (32.3%), comparable for smokers and non-smokers; clusters of calcified small pulmonary nodules in 9 (6.6%); and cavitated nodules in 4 (2.9%). Histologic examination of surgical samples found arterial abnormalities, emphysema with alveolar ruptures in 3, accompanied by diffuse hemorrhage and increased hemosiderin resorption.

Conclusion In vEDS patients, identification of lung parenchymal abnormalities is common on CT. The most frequently observed CT finding was emphysema suggesting alveolar wall rupture which might facilitate the diagnostic screening of the disease in asymptomatic carriers of a genetic *COL3A1* gene mutation. The prognostic value and evolution of these parenchymal abnormalities remain to be evaluated.

Key Points

- *Patients with vEDS can have lung parenchymal changes on top of or next to thoracal vascular abnormalities and that these changes can be present in asymptomatic cases.*
- *The presence of these parenchymal changes is associated with a slightly higher incidence of respiratory events (although not statistically significant).*
- *Identification of the described CT pattern by radiologists and chest physicians may facilitate diagnostic screening.*

Keywords Ehlers–Danlos syndrome · Hemothorax · Pneumothorax · CT scan · Pulmonary emphysema

Abbreviations

ADE	Advanced destructive emphysema
BMI	Body mass index
CLE	Centrilobular emphysema
HRCT	High-resolution computed-tomography
ins/del/dup	Insertions/deletions/duplications
PACS	Picture-archiving and communication system
PSE	Paraseptal emphysema
vEDS	Vascular Ehlers–Danlos syndrome

✉ Samia Boussouar
samia.boussouar@aphp.fr

Extended author information available on the last page of the article

Vascular Ehlers–Danlos syndrome (vEDS), a rare genetic disease with an autosomal-dominant trait, is caused by pathogenic variants within the collagen type III alpha-1 chain (*COL3A1*) gene. The resulting quantitative and qualitative alterations in type III collagen, typically lead to organ fragility,

expressed clinically in young adults as arterial dissections and ruptures, bowel perforation, gravid uterine, and organ ruptures [1–4].

The premature death of patients with vEDS syndrome is frequently related to spontaneous rupture of arterial aneurysms and/or dissections. These arterial lesions are frequent and always looked for in the CT scan performed in case of complication or in case of screening during the monitoring of these patients. Arterial lesions are most often localized on the branches of the abdominal aorta and supra-aortic branches. Pulmonary vascular segment involvement is very rare [5, 6].

Furthermore, chest involvement, manifesting as hemo-/pneumothoraces and pulmonary hemorrhages, is not uncommon in vEDS patients, but has not been formally characterized in a large patient cohort. Indeed, pulmonary involvement and parenchymal disease were identified only in case reports and case-series describing cysts, intra-pulmonary cavitary lesions, and interstitial disease [7–17].

To further document pulmonary disease in vEDS, a study on clinical and CT imaging of lung involvement was undertaken in a large series of consecutive vEDS patients, with corresponding histology when available.

Methods

Population

All patients with molecularly confirmed vEDS referred, between 2004 and 2016, to the French National Referral Centre for Rare Vascular Diseases were included in this retrospective cohort study when CT scans had been obtained for either symptom (index cases) or screening after genetic diagnosis (relatives). All vEDS-related symptoms, clinical characteristics (smoker status, body mass index (BMI; kg/m^2), and history of respiratory events) were collected in a dedicated database with systematic follow-up.

Respiratory events were assessed from the initial evaluation to the last follow-up visit to our institution. Respiratory events were defined as pneumothorax, hemothorax, or hemoptysis.

Genetic testing and the database were managed in compliance with the French legislation (French Bioethics Law no. 2004–800), and written informed consent was obtained from all patients. As reported previously [18], based on the results of *COL3A1*-mutation screening, distinct variants were divided into three groups as follows: glycine substitutions, splice-site and in-frame insertions-deletions/duplications (ins/ del/dup), and variants leading to haplo-insufficiency.

Chest CT scans

CT acquisitions were performed using either a 4-row or 64-row CT system (General Electrics) in the cephalocaudal direction from the lung apex to the ischial tuberosity to include fully the chest, abdomen, and pelvis. The patients were instructed to hold their breath during scanning. In all cases, image acquisition was done during the arterial phase after an intravenous bolus injection of 350 g/L of iodinated contrast material at a rate of 3.5 mL/s, in accordance with an institutionally defined protocol optimized to screen for vEDS arterial lesions. The volume of contrast medium to be injected was calculated based on the patient's body weight, with the total dose ranging from 80 to 130 mL; it was followed by a 50-mL saline flush at 3.5 mL/s. The exposure parameters for the CT scans were as follows: 80 to 120 kVp, 50 to150 mA with dose modulation (angular and z). Axial chest images were reconstructed with 0.625- to 1.2-mm slice thickness, high resolution and soft tissue algorithms, and an optimized field of view of 25 to 30 cm.

All chest CT images were retrieved from the institution's picture-archiving and communication system (PACS) to be analyzed on a dedicated workstation with both mediastinal (level and width = 50 Hounsfield units (HU) and 400 HU, respectively) and lung window settings (level and width = −600 HU and 1500 HU, respectively). Minimum- and maximum-intensity projection algorithms were applied to each set of CT scans with 5-mm slice thickness to facilitate detection of nodules and hypodense structures (width 500 HU; level − 950 HU).

Two chest radiologists (S.B. and P.A.G.) blinded to clinical data conducted a consensus review chest CT scans performed either on a systematic basis or because of respiratory events occurring during follow-up. Only the first HRCT examination systematically obtained for each vEDS patient at our institution or scans obtained because of respiratory events occurring during follow-up were analyzed herein. To clarify the anatomic distribution of abnormalities, the lungs were divided into axial upper and lower zones at the level of the tracheal carina. The presence and distribution of the following features were defined according to the last Fleischner Society statement [19]. *Centrilobular emphysema* (CLE) was considered to be small poorly or well-defined areas of low attenuation surrounded by normal lung without visible walls. *Advanced destructive emphysema* (ADE), representing advanced CLE, was defined as a generalized decrease of lung attenuation without focal hypoattenuation. Interlobular septa were often preserved and splayed, facilitating the identification of pulmonary lobular hyperexpansion. In addition, the central pulmonary vessels were often distorted, splayed, and narrowed with decreased branching (architectural distortion). *Paraseptal emphysema* (PSE) was defined as subpleural and peribronchovascular foci of low attenuation separated by intact interlobular septa thickened by associated mild fibrosis. For regions of low attenuation adjacent to visceral pleura, PSE may be further classified as peripheral, mediastinal, diaphragmatic, or fissural. *Bullae* were defined as avascular low-

attenuation areas, > 1 cm in diameter, with a thin but visible wall. *Pulmonary cyst* was a round parenchymal lucency or a low-attenuation area delimited by a well-defined interface with the normal lung. *Nodule* corresponded to a poorly or well-defined rounded opacity, measuring up to 3 cm in diameter, with homogenous soft tissue attenuation. *Cavitary lesions* were either gas-filled spaces or low-attenuation areas associated with a > 4-mm-thick wall within pulmonary consolidation, within a mass or a nodule.

Vascular abnormalities were assessed like thoracic arterial aneurysm/dissections.

The Haller index was defined as the ratio of the transverse diameter (the horizontal distance of the inside of the ribcage) to the anteroposterior diameter (the shortest distance between the vertebrae and sternum) [20].

Histology

Because of respiratory events requiring surgery, five histologic samples from four different patients were available and could be analyzed using previously described criteria [21], and others, such as pleural thickening and tobacco-induced changes. The histologic findings of these samples were compared to those obtained in five control subjects, who had undergone lung surgery for recurrent pneumothoraces. For each patient, three or four representative 4-μm-thick tissue samples were examined after staining with hematoxylin, eosin and saffron, Sirius red, and iron staining. Two independent pathologists blinded to patient status conducted the histologic examinations using previously described criteria [21].

Statistical analyses

Quantitative variables are expressed as mean ± standard deviation or median (interquartile range). Quantitative variables were compared with unpaired *t* tests or Mann–Whitney tests and qualitative variables with chi-square with Yates correction or Fisher's exact tests when appropriate. Variables associated with an abnormal CT scan at the 10% level ($p \leq 0.10$) were then introduced into a multivariable logistic regression model. Statistical analyses were performed using R (https://www.R-project.org/) software. $p \leq 0.05$ defined significance.

Results

Patients and clinical characteristics

Among 138 vEDS patients eligible to participate between April 2004 and February 2016, two were excluded because of breathing artifacts impacting the analysis of lung CT images. Clinical characteristics and genotypes of the 136 analyzed patients, including 86 index cases and 50 first-degree relatives, are reported in Table 1. Their mean age was 37 ± 13 years, 83/136 (61%) were women, and 50/136 (36.8%) were current (n = 30) or former (n = 20) smokers with an average exposure of 12 pack-years. Among identified pathogenic variants, glycine substitutions within the triple helix domain predominated, followed by splice-site variants and in-frame insertions-deletions, and variants leading to haploinsufficiency.

Seven out of 136 (5.1%) patients had an associated respiratory disease (asthma (n = 2) or sarcoidosis (n = 2), pulmonary embolism (n = 1), sleep-apnea syndrome (n = 1), and bronchial cancer (n = 1)). Before and during the study period, 24/136 (17.6%) patients developed respiratory events, mainly pneumothorax (n = 17), and several with hemothorax (n = 4) or hemoptysis (n = 3); 11 of them required thoracic surgery. For the prior and current respiratory event (n = 24), 20 were index cases and 4 were related cases.

Imaging findings

Chest CT scans were performed in 125 vEDS patients at the initial evaluation in our institution and in 11 patients because of clinical events occurring during follow-up. Six patients had CT images obtained for acute chest events, pneumothorax (n = 1), pulmonary hemorrhage (n = 1), hemopneumothorax (n = 2) (Fig. 1), or pleural effusions related to vascular dissection (n = 2). Five patients had acute clinical events related to sub-diaphragmatic vascular dissections without thoracic consequences. No vascular abnormalities were found.

Comparisons of patients' clinical characteristics according to the presence or absence of CT pulmonary abnormalities are reported in Table 2. An abnormal chest CT scan included all parenchymal and pleural abnormalities. Chest CT scans were abnormal for 78/136 (57.4%) patients. The two groups did not differ significantly for age, sex, weight, genotype, or smoking history. However, patients with pulmonary abnormalities were significantly taller. In multivariate analysis, the height remained significantly higher in abnormal CT groups (OR = 1.08, IC95% [1.02–1.15], p = 0.01). Fifty-nine patients who did not present respiratory symptoms or prior respiratory event had abnormal chest CT findings. Two patients with no parenchymal changes on CT had a pneumothorax. The incidence of pneumothorax was significantly higher in the group with parenchymal abnormalities. Among chest CT characteristics (Table 3), emphysema was the most frequent abnormality, observed in 44/78 (56.4%) patients, followed by linear opacities connected to pleura observed in 28/78 (35.8%), clusters of calcified micronodules in 9/78 (11.5%) (Fig. 2a), and cavitating nodules in 4/78 (5.1%) (Fig. 2b). One patient developed interstitial pneumonitis (peribronchovascular consolidation compatible with organizing pneumonia) and another had small nodules related to sarcoidosis. Three patients had a thick apical cap, two patients had ground-glass areas, and one

Table 1 Demographics of 136 subjects with vEDS (n = 136)

Characteristic	All subjects
Index cases/relatives, no.	86/50
Age, years	37 ± 13
Male/female	53 (39)/83 (61)
Height, cm	165.8 ± 9.3
Weight, kg	61.4 ± 12.6
Body mass index, kg/m^2	22.3 ± 3.9
Smoking status	
Active or ex-smoker	50 (36.7)
Pack-years	12 ± 7
Never smoker	86 (63.2)
Genotype	
Glycine substitution	83 (61)
Splice/Ins/Del/Dup	42 (30.9)
Haplo-insufficiency	11 (8.1)
Prior and current respiratory event	24 (17.6)
Pneumothorax	17 (12.5)
Hemothorax	4 (2.9)
Hemoptysis	3 (2.2)
Prior thoracic surgery	11 (8.1)

Results are expressed as no. (%) or mean ± SD, unless stated otherwise

patient had small nodular ground-glass opacities mainly in the upper lobes. Emphysema was centrilobular in all patients with emphysema, and paraseptal in 22/44 (62.2%) (Fig. 3). CLE was about equally frequent in the upper and lower lobes. PSE was seen, in decreasing frequency, along the peripheral, mediastinal, diaphragmatic, or fissural pleura. Peribronchovascular paraseptal emphysema was found, but less often. Four patients had ADE in the lower lung zones (Fig. 4). Linear opacities connected to pleura (Figs. 4 and 5) were mostly connected to the diaphragmatic, but less frequently to mediastinal or fissural pleura. The mean Haller index was 2.34 ± 0.52.

CLE and PSE were identified in 21/50 (42%) smokers and 23/86 (6.7%) non-smokers. Emphysema distribution in the upper or lower lobes, linear opacities connected to pleura, clusters of calcified small nodules, cavitating nodules, and Haller index did not differ between smokers and non-smokers (Table 4). Subanalysis on lung abnormalities on CT did not show statistical difference between the different types of COL3A1 variants (Table 2).

Histologic findings

Histologic examination findings are summarized in Table 5. Emphysema lesions were found in three patients with ruptured alveoli, accompanied by diffuse pleural scarring or localized pleural fibrosis. The peribronchovascular emphysema seen in histologic findings (Fig. 6a, b) in our series could correspond to the emphysema seen on CT scan. Fibrous nodules and calcifications/ossifications were not observed in the examined specimens (in our series). vEDS patients 2 and 4 had a very specific pattern of diffuse hemorrhage. Hemosiderin resorption was particularly notable in patient 4, accompanied by alveolar wall thickening, probably secondary to chronic intra-alveolar hemorrhage. Pulmonary arteries in vEDs patients were more irregular and thin-walled, with more diffuse hemorrhage and hematomas, than in controls (Fig. 6c, d). No intraluminal outgrowth was observed.

Discussion

Herein, we described a large cohort of vEDS patients with long-term follow-up, their clinical presentations, and CT imaging of disease-related pulmonary involvement, with corresponding histologic findings for a few of them. This is the largest cohort of vEDS patients, whose frequencies of pulmonary lesions were routinely analyzed without selection bias. Lung CT abnormalities were not influenced by types of *COL3A1* variants. Types of COL3A1 variants have been shown to have significant influence on the onset of arterial and digestive complications, as well as on overall mortality. Indeed, patients with splice-site variants seem to develop organ complications earlier and have a higher mortality rate at a given age than patients with glycine substitutions. The patients with the latest onset of complications are patients with variants leading to haplo-insufficiency, typically coming to

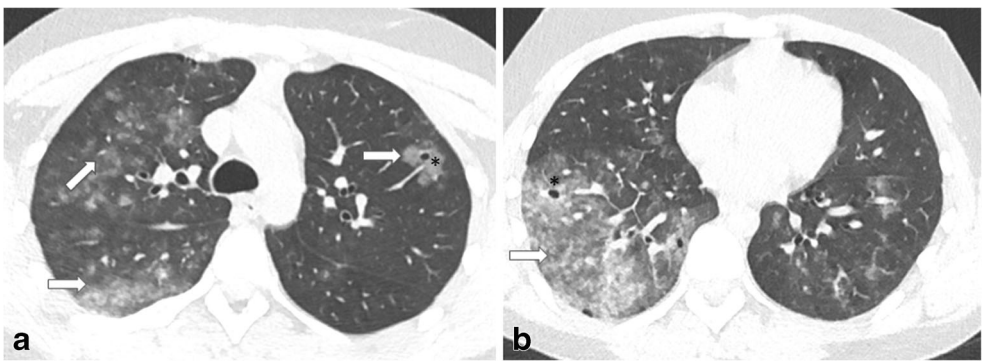

Fig. 1 Axial thin-section CT images (**a**, **b**) in the lung window of a 48-year-old male non-smoker with vEDS, showing diffuse round-glass opacities, suggestive of pulmonary hemorrhage, and some low-attenuation areas (asterisk)

Table 2 Comparison of clinical and genetic characteristics according to CT scan abnormalities in vEDS

Characteristic	Normal CT	Abnormal CT	*p* value*
Number	58	78	
Age, years	37.3 [26.6–43.9]	36.3 [27.8–43.4]	.995
Male/female, no.	18/40	35/43	.102
Weight, kg	58.0 [51.0–70.0]	60.0 [54.0–66.0]	.705
Height, cm	163.0 [156.0–169.0]	167.0 [160.0–174.0]	.030
Body mass index, kg/m^2	22.5 [20.0–25.1]	21.0 [19.3–23.4]	.143
Genotype			.772
Glycine substitution	37 (63.8)	46 (59.0)	.569
Splice/Del/Ins (splice/del/ins/dup)	16 (27.6)	26 (33.3)	.473
Haplo-insufficiency	5 (8.6)	6 (7.7)	1.000
Smoking status			.495
Never	39 (67.2)	48 (61.5)	
Current	10 (17.2)	20 (25.6)	
Former	9 (15.5)	10 (12.8)	
Pack-years; median [IQR]	8 [5.0–10.0]	12 [6–17]	.531
Haller index	2.4 ± 0.6	2.3 ± 0.4	.123
Prior respiratory event	2 (3.4)	22 (28.2%)	18×10^{-4}
Pneumothorax	2 (3.4)	15 (19.2)	.006
Hemothorax	0	4 (5.1)	.136
Hemoptysis	0	3 (3.8)	.261
Chest surgery	1 (1.7)	10 (12.8)	.042

Results are expressed as no. (%) or mean ± SD, unless stated otherwise

*Considered statistically significant from emphysema-like group with a *p* value threshold < 0.05

medical attention a median 12 to 21 years later than patients with glycine substitutions and splice-site variants, respectively. In this study, lung CT abnormalities were not influenced by types of COL3A1 variants, and more interestingly, patients with haplo-insufficiency had similar prevalence of CT abnormalities than the more severe glycine and splice-site variants. In contrast to the literature [3], we did not find more pectus excavatum in this population of vEDS patients. The normal Haller index indicated the absence of a link between parenchymal abnormalities and morphology of the thoracic cavity. In histologic finding, pleural thickening is probably the consequence of the presence of hemorrhage that limits resorption [22]. Dar et al reported a vEDS case presenting with hemoptysis and hemopneumothorax and described increased fibrosis on the pleural surface with an increased vascularity on surgical lung biopsy [13].

We did not find any cysts, since the low-attenuation areas in the lung parenchyma without visible walls corresponded to emphysema, as confirmed by the histologic examinations of five samples. The notion of cysts in journals is based on a few reported cases [23, 24]. Therefore, by analyzing thin-section chest CT images, vEDS can be differentiated from cystic lung diseases, which can be responsible for familial spontaneous pneumothorax in several genetic diseases, including sporadic or tuberous sclerosis complex-associated lymphangioleiomyomatosis, α_1-antitrypsin deficiency, Marfan syndrome, Birt-Hogg-Dubbé syndrome, and cystic fibrosis [23, 24].

Among pulmonary lesions described in detail in our series, there was no finding of underlying interstitial lung disease or fibrosis as well on CT scan as on histologic findings. Chest CT abnormalities concerned only emphysema, linear bands, cavitating nodules, and clusters of calcified micronodules.

The presence of emphysema in this disease was previously described in a case report [9] and eight of nine vEDS patients included in a histopathology study [21]. Although tobacco smoking is the cardinal risk factor for centrilobular emphysema, 64% of our patients had never smoked. Hence, tobacco was not statistically related to the presence of emphysema and distribution. Compared to smaller series of vEDS patients [1, 3], pneumothorax (12.5%) and hemothorax (3%) frequencies were very similar.

The mechanism of emphysema onset and its development in vEDS is still unclear. Dilacerations of the alveolar wall could be one of the underlying mechanisms. Kawabata et al argued that fragility of the alveolar wall, which contains type III collagen, can also be responsible for other pathologies associated with parenchymal and pleural damage [21]. Corrin et al also suggested that spontaneous tearing might cause pulmonary emphysema formation in vEDS patients [25], with spontaneous laceration of lung tissue being the key

Table 3 Chest CT findings of the 136 Subjects with vEDS

HRCT characteristic	Value*
Emphysema	44 (32.4)
Centrilobular	42 (30.9)
< 1 cm	42 (30.9)
Confluent centrilobular emphysema	7 (5.1)
Upper distribution	30 (22.1)
Lower distribution	34 (25)
Paraseptal	30 (22.1)
Diameter < 1 cm	22 (16.2)
Bullae (diameter > 1 cm)	14 (10.3)
Peripheral	27 (19.9)
Mediastinal	13 (9.6)
Fissural	11 (7.4)
Diaphragmatic	12 (8.8)
Peribronchovascular	9 (6.6)
Advanced destructive	4 (2.9)
Upper	0
Lower	4 (2.9)
Linear opacities connected to pleura	28(20.5)
Diaphragmatic	28 (20.5)
Mediastinal	4 (2.9)
Fissural	3 (2.2)
Clusters of calcified small nodules	9 (6.6)
Cavitating nodules	4 (2.9)
Haller index	2.36 [1.53–5.35]

*Values are expressed as no. (%) or median [interquartile range]

pathological feature. According to this mechanical hypothesis, it is not surprising to observe in our vEDS patients an alveolar rupture distribution which predominates at the level of alveolar attaches to subpleural and peribronchiolar conjonctive tissue, instead of being panlobular. Our findings also support the hypothesis that abnormalities might not be the cause, but rather the consequence of an event and might be the residual scar of a past respiratory event. Linear opacities connected to pleura were also found in 28 (20.6%) of our patients, mainly diaphragmatic, representing a previously undescribed feature of this disease. Linear opacities probably represent atelectasis or interlobular septa adjacent to the emphysematous spaces. Atelectasis may be secondary to pleural fibrosis, since it was also seen in histologic specimens. These lines may represent connected thickened interlobular septa made more conspicuous by extensive adjacent parenchyma destruction. [26–29]

The third abnormality found in our study was cavitating nodules with similar observations made in some case reports [30, 31]. These probably correspond to hematomas caused by spontaneous arteriolar ruptures. Because of blood-vessel fragility and abnormal connective tissue repair of hemorrhagic foci, hematomas shrink to ultimately evolve into fibrous nodules.

According to the largest pleuropulmonary histopathology series of vEDS cases reported to date, eight of nine patients had fibrous nodules, six of them with ossifications probably explained by osseous metaplasia found within these fibrous nodules [21]. The same mechanism probably explains the multiple calcified micronodules seen in nine of our patients.

We also compared CT and histologic findings. No cysts were seen. Smokers and non-smokers had emphysema. The results of the histologic analysis suggest that emphysema is an indicator of alveolar rupture and perforated nodules would indicate hematomas. The cause of these abnormalities is a matter of speculation but we advance that these abnormalities seem to resemble thoracic pulmonary blast. Pulmonary blast lesions are due to the impact of a pressure wave on the chest wall with hyperpressure in the airways followed by a secondary depression wave. The main anatomic injuries seen after a blast explosion are pneumothorax, pneumatocele, hematopneumatocele, and alveolar rupture [32], i.e., the same chest injuries seen in vEDS. A pathophysiological mechanism could perhaps be the greater sensitivity to air-pressure waves in vEDS.

This study has several limitations. First is its retrospective nature with no pulmonary function tests for comparison with CT abnormalities. Because we included asymptomatic cases, missing pulmonary function tests is unavoidable in routine practice. In addition, we only analyzed the patients' first chest

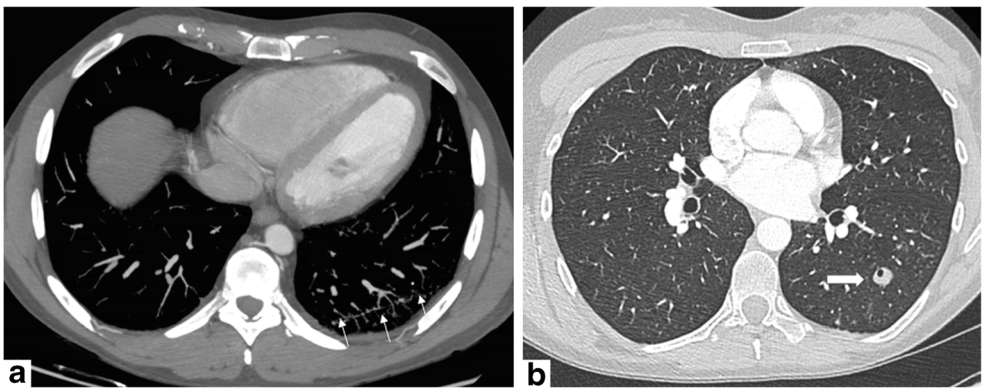

Fig. 2 **a** Multiple calcified micronodules in the left lower lobe (arrows) in a 38-year-old female non-smoker with vEDS (axial 5-mm maximum-intensity projection). **b** Cavitating nodule in the left lower lobe of a 28-year-old female non-smoker with vEDS

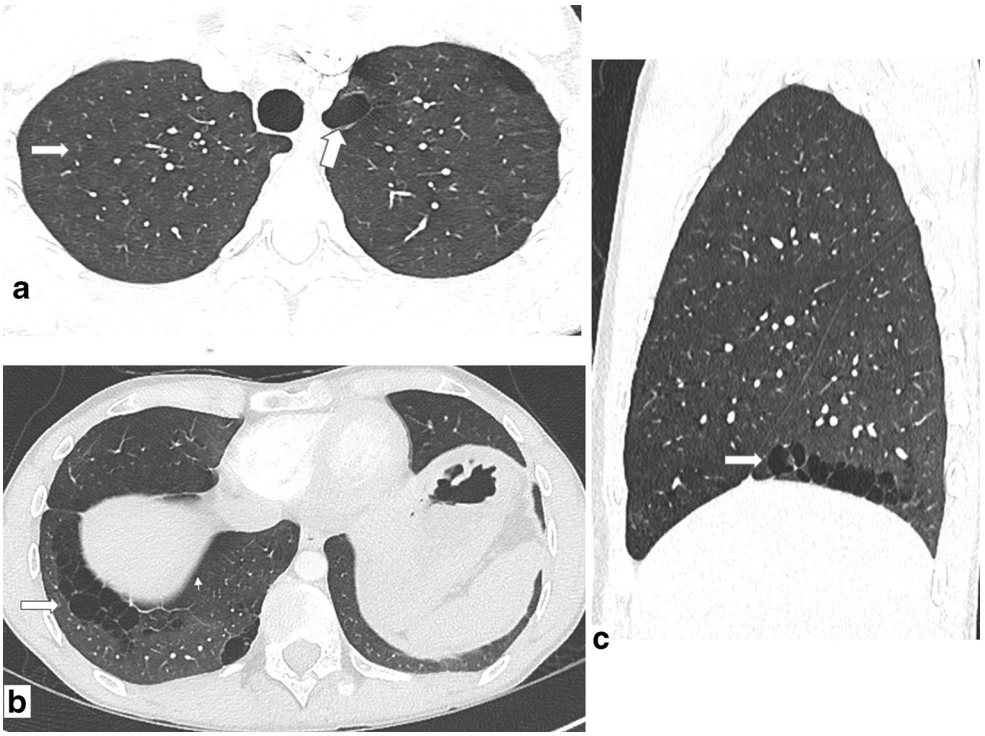

Fig. 3 Thin-section CT images of a 21-year-old male non-smoker with vEDS. Reformatted axial (**a**, **b**) and sagittal images of the right lung (**c**). Multiple paraseptal emphysematous spaces in the apex of the left upper lobe (**a**) and the lung bases of the right lung (particularly along the diaphragm) (**b**, **c**). Note the presence of several small nodular round-glass opacities in the upper lobes (**a**, **c**)

CT scans to determine whether or not they were normal. Although unlikely, lung parenchymal changes could be due to other concomitant lung diseases. Further studies are needed to analyze the evolution of the lung parenchyma under treatment in this context and its potential link with vascular disease. Emphysema is not specific; however, in young patients or non-smokers, it could be indicative. Emphysema has been reported in other genetic diseases. Several syndromes, such as cutis laxa, Niemann-Pick disease, and telomeropathies, are related to emphysema. Genome-wide association studies demonstrated that several genes are associated with emphysema on CT [33]. Emphysema associated with alpha-1-antitrypsin

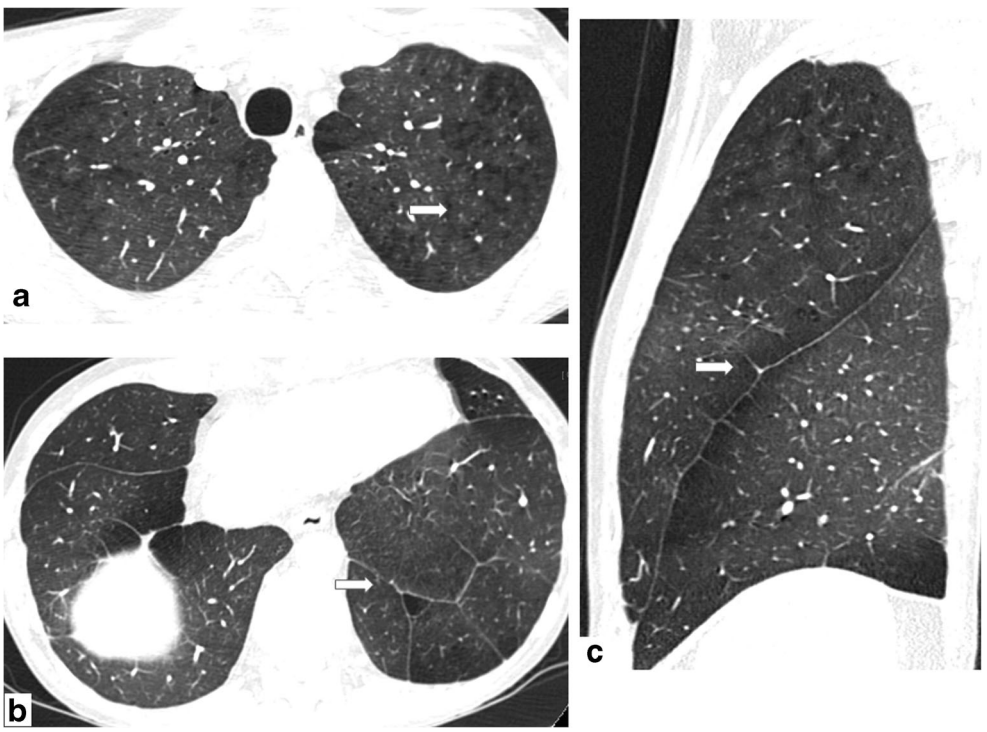

Fig. 4 Axial thin-section CT images in the upper (**a**) and the lower (**b**) lung zones, and reformatted right sagittal image (**c**) of a 38-year-old male non-smoker with vEDS. Note the presence of centrilobular emphysema in the upper lobes (**a**), and paraseptal emphysema along the fissures and the diaphragmatic pleura. Linear opacities are connected to the diaphragmatic pleura and fissures (arrows)

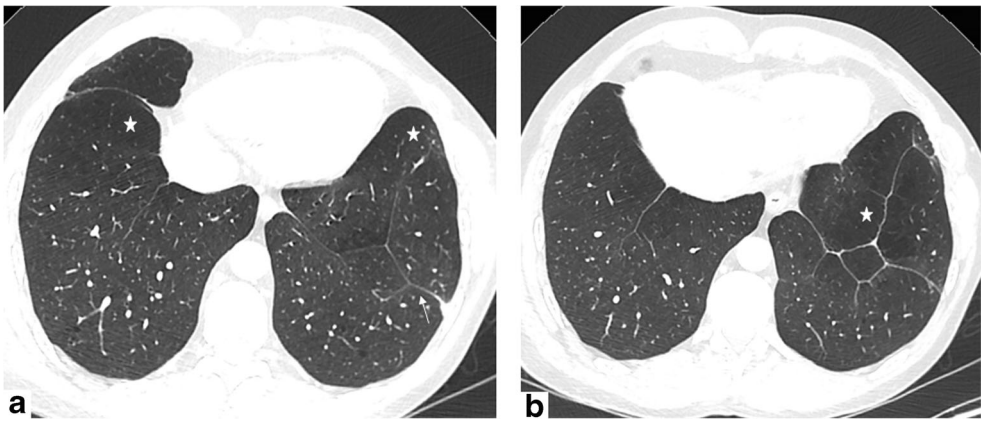

Fig. 5 **a**, **b** Axial thin-section CT images through the lung bases of a 40-year-old male non-smoker with vEDS. Note the areas of advanced destructive emphysema in the anterobasal segment of the lower lobes and linear opacities through the left lung bases (asterisk)

Table 4 CT Findings according to smoker status in subjects with vEDS

Characteristic	Non-smokers (n = 86)	Smokers (n = 50)	p value
Age, years	35.9 ± 14.2	35.2 ± 12.1	0.4607
Weight, kg	60.2 ± 11	63.1 ± 14	0.2151
Height, cm	164 ± 8.7	169 ± 8.7	0.0006
Body mass index, kg/m^2	22.5 ± 3.9	22.0 ± 3.9	0.4611
Female/male, no.	62/24	21/29	0.0005
Lung disease	3 (3.5)	6 (12)	0.4225
Respiratory event	17 (19.8)	12 (24)	0.5612
HRCT			
Emphysema	23 (26.7)	21 (42)	0.1707
Centrilobular	23 (26.7)	19 (38)	0.1707
Diameter < 1 cm	23 (26.7)	19 (38)	0.6444
Confluent centrilobular emphysema	5 (5.8)	2 (4)	0.08857
Upper distribution	15 (17.4)	15 (30)	0.8373
Lower distribution	21 (24.4)	13 (26)	0.966
Paraseptal	18 (20.9)	12 (24)	0.6772
Diameter < 1 cm	14 (16.3)	8 (16)	0.6177
Bullae	8 (9.3)	6 (12)	0.6322
Peripheral	16 (18.6)	11 (22)	0.2287
Mediastinal	6 (7)	7 (14)	0.7453
Fissural	7 (8.1)	3 (6)	0.7963
Diaphragmatic	8 (9.3)	4 (8)	0.485
Peribronchovascular	7 (8.1)	2 (4)	0.6247
Advanced destructive	2 (2.3)	2 (4)	0.1707
Upper	0	0	
Lower	2 (2.3)	2 (4)	0.6247
Linear opacities connected to pleura	17(19.8)	11 (22)	0.7562
Diaphragmatic	17 (19.8)	11 (22)	0.7562
Mediastinal	4 (476)	0	0.2963
Fissural	3 (3.5)	0	0.2974
Clusters of calcified small nodules	7 (8.1)	2 (4.0)	0.3491
Cavitating nodules	2 (2.3)	2 (4.0)	0.5774
Haller index	2.4 ± 0.5	2.3 0.4	0.4509

Values are expressed as no. (%) or mean ± standard deviation

Table 5 Pleuropulmonary histology in 5 sample from 4 subjects with vEDS

Histology	Patient 1		Patient 2	Patient 3	Patient 4
Sex/Age (years)	M/21	M/27	M/17	F/25	M/17
Respiratory event	Pneumothorax	Pneumothorax	Giant bubble excised	Pneumothorax	Resected cystic lesion with cavitation
Emphysema	++	++	0	+	+
Hemorrhagic bullae	–	–	+	–	+
Diffuse fibrous pleural thickening	+	+	+	++	–
Bronchiolar inflammation	–	–	++	–	+
Tobacco-induced changes	++	+	–	–	–
Congestive pattern	–	–	+	–	++
Anomalies/ruptured arteries	+	+	+	+	+
Focal hemorrhage	–	+	–	–	–
Diffuse hemorrhages	–	+	+++	–	+++
Hemosiderosis	+	+	++	–	++

deficiency is panlobular, characterized by uniform destruction of the pulmonary lobule leading to widespread areas of abnormally low attenuation without visible walls, and in contrast to CLE, the destruction is generalized and more prominent in the lower lobes. Emphysema in non-smokers has also been reported in patients with connective tissue diseases [34] but always in association with lung fibrosis [35, 36].

In conclusion, based on a large cohort of patients with molecularly confirmed vEDS, we were able to identify different previously undescribed pulmonary lesions and report their frequencies. The most common CT feature, including in clinically asymptomatic patients, was emphysema, suggesting alveolar wall ruptures. Identification by radiologists of this unexpected pulmonary pattern in seemingly healthy young

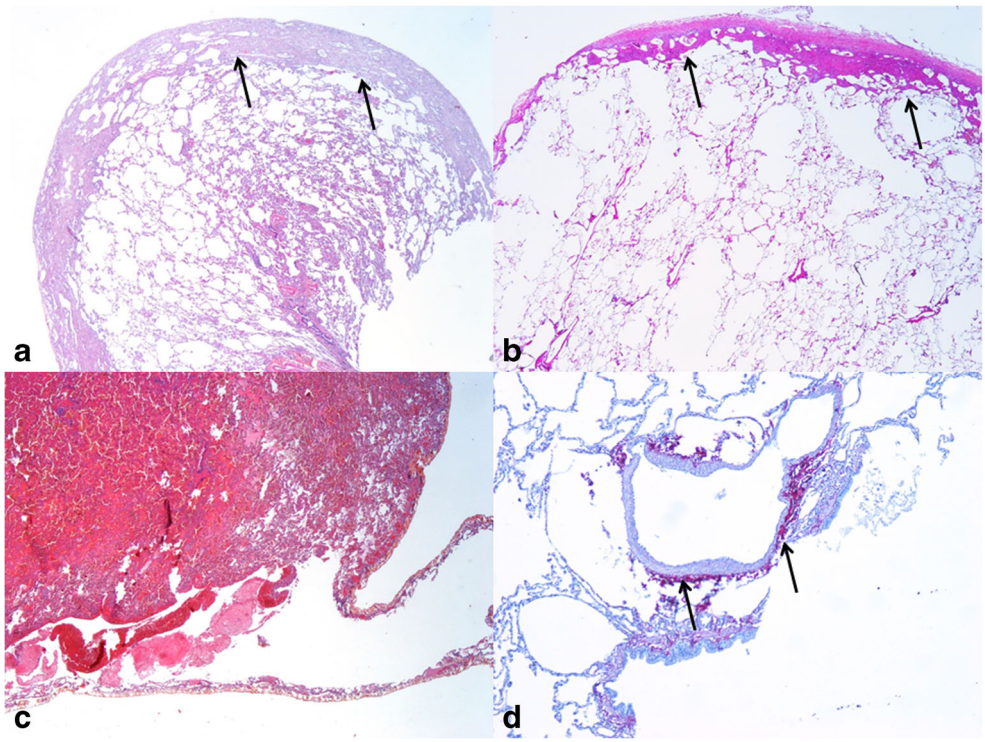

Fig. 6 Examples of histology of lung sections in vEDS. **a**, **b** Hemalun Eosine Saffron (HES) stain demonstrating emphysematous changes in the first (**a**) and second (**b**) samples of case 1. Note the diffuse pleural thickening (black arrows, × 2 and × 4 magnification). **c** Hemorrhagic bullae. Sirius red–stained histologic sections on the second resection at 27 years old (**d**), demonstrating the arterial thickness variations (arrows) commonly seen in vEDS (× 20 magnification)

subjects without known vEDS should trigger diagnostic investigations. The prognostic value and evolution of these parenchymal abnormalities remain to be characterized. We also need to determine to what extent these CT findings are associated with respiratory or other arterial events and outcomes.

Acknowledgements Two of the authors of this publication are members of the European Reference Network on Rare Multisystemic Vascular Diseases (VASCERN) - Project ID: 769036.

Funding The authors state that this work has not received any funding.

Declarations

Conflict of interest The authors of this manuscript declare no relationships with any companies whose products or services may be related to the subject matter of the article.

Statistics and biometry Two of the authors have significant statistical expertise.

Informed consent Written informed consent was waived by the Institutional Review Board.

Ethical approval Institutional Review Board approval was obtained.

This study was formally approved by the comité de protection des personnes Ile de France II (IRB registration#: 00001072).

Methodology
- retrospective
- observational
- multicenter study

References

1. Byers PH, Belmont J, Black J et al (2017) Diagnosis, natural history, and management in vascular Ehlers-Danlos syndrome. Am J Med Genet C Semin Med Genet 175:40–47
2. Frank M, Albuisson J, Ranque B et al (2015) The type of variants at the *COL3A1* gene associates with the phenotype and severity of vascular Ehlers-Danlos syndrome. Eur J Hum Genet 23:1657–1664
3. Oderich GS, Panneton JM, Bower TC et al (2005) The spectrum, management and clinical outcome of Ehlers-Danlos syndrome type IV: a 30-year experience. J Vasc Surg 42:98–106
4. Pepin M, Schwarze U, Superti-Furga A, Byers PH (2000) Clinical and genetic features of Ehlers-Danlos syndrome type IV, the vascular type. N Engl J Med 342:673–680
5. Chu LC, Johnson PT, Dietz HC et al (2012) Vascular complications of Ehlers-Danlos syndrome: CT findings. AJR Am J Roentgenol. 198(2):482–487
6. Zilocchi M, Macedo TA, Oderich GS, Vrtiska TJ, Biondetti PR, Stanson AW (2007) Vascular Ehlers-Danlos syndrome: imaging findings. AJR Am J Roentgenol 189(3):712–719
7. Dowton SB, Pincott S, Demmer L (1996) Respiratory complications of Ehlers-Danlos syndrome type IV. Clin Genet 50:510–514
8. Hatake K, Morimura Y, Kudo R, Kawashima W, Kasuda S, Kuniyasu H (2013) Respiratory complications of Ehlers-Danlos syndrome type IV. Leg Med (Tokyo) 15:23–27
9. Ishiguro T, Takayanagi N, Kawabata Y et al (2009) Ehlers-Danlos syndrome with recurrent spontaneous pneumothoraces and cavitary lesion on chest X-ray as the initial complications. Intern Med 48: 717–722
10. Nakagawa H, Wada H, Hajiro T et al (2015) Ehlers-Danlos syndrome type IV with bilateral pneumothorax. Intern Med 54:3181–3184
11. Abrahamsen BJ, Kulseth MA, Paus B (2015) A 19-year-old man with relapsing bilateral pneumothorax, hemoptysis, and intrapulmonary cavitary lesions diagnosed with vascular Ehlers-Danlos syndrome and a novel missense mutation in *COL3A1*. Chest. 147:e166–e170
12. Yost BA, Vogelsang JP, Lie JT (1995) Fatal hemoptysis in Ehlers-Danlos syndrome. Old malady with a new curse. Chest 107:1465–1467
13. Dar RA, Wani SH, Mushtaque M, Kasana RA (2012) Spontaneous hemo-pneumothorax in a patient with Ehlers-Danlos syndrome. Gen Thorac Cardiovasc Surg 60:587–589
14. Murray RA, Poulton TB, Saltarelli MG et al (1995) Rare pulmonary manifestation of Ehlers-Danlos syndrome. J Thorac Imaging 10: 138–141
15. Selim B, Lane CR, Rubinowitz AN, Siner JM (2010) Spontaneous hemothorax and recurrent hemoptysis in a 26-year-old man with skin lesions. Chest. 37:480–483
16. Shields LB, Rolf CM, Davis GJ, Hunsaker JC III (2010) Sudden and unexpected death in three cases of Ehlers-Danlos syndrome type IV. J Forensic Sci 55:1641–1645
17. Watanabe A, Kawabata Y, Okada O et al (2002) Ehlers-Danlos syndrome type IV with few extrathoracic findings: a newly recognized point mutation in the *COL3A1* gene. Eur Respir J 19:195–198
18. Frank M, Adham S, Seigle S et al (2019) Vascular Ehlers-Danlos syndrome: long-term observational study. J Am Coll Cardiol 73: 1948–1957
19. Lynch D, Austin JH, Hogg JC et al (2015) CT-definable subtypes of chronic obstructive pulmonary disease: a statement of the Fleischner society. Radiology. 277:192–205
20. Poston PM (2015) The case for using the correction index obtained from chest radiography for evaluation of pectus excavatum. J Pediatr Surg 5:1940–1944
21. Kawabata Y, Watanabe A, Yamaguchi S et al (2010) Pleuropulmonary pathology of vascular Ehlers-Danlos syndrome: spontaneous laceration, haematoma and fibrous nodules. Histopathology. 56:944–950
22. Jantz A, Veena B (2006) Pleural fibrosis. Clin Chest Med 27(2): 181–191
23. Ryu JH, Swensen SJ (2003) Cystic and cavitary lung diseases: focal and diffuse. Mayo Clin Proc 78:744–752
24. Raoof S, Bondalapati P, Vydyula R et al (2016) Cystic lung diseases: algorithmic approach. Chest. 150:945–965
25. Corrin B, Simpson CG, Fisher C (1990) Fibrous pseudotumours and cyst formation in the lungs in Ehlers-Danlos syndrome. Histopathology. 17:478–479
26. Copley SJ, Wells AV, Müller NL et al (2002) Thin-section CT in obstructive pulmonary disease: discriminatory value. Radiology. 223:812–819
27. Smith BM, Austin JH, Newell JD Jr et al (2014) Pulmonary emphysema subtypes on computed tomography: the MESA COPD study. Am J Med 127:94.e7–94.23
28. Takahashi M, Fukuoka J, Nitta N et al (2008) Imaging of pulmonary emphysema: a pictorial review. Int J Chron Obstruct Pulmon Dis 3:193–204
29. Stern EJ, Frank MS (1994) CT of the lung in patients with pulmonary emphysema: diagnosis, quantification, and correlation with pathologic and physiologic findings. AJR Am J Roentgenol 162: 791–798
30. Herman TE, McAlister WH (1994) Cavitary pulmonary lesions in type IV Ehlers-Danlos syndrome. Pediatr Radiol 24:263–265

31. Berezowska S, Christe A, Bartholdi D, Koch M, von Garnier C (2018) Pulmonary fibrous nodule with ossifications may indicate vascular Ehlers-Danlos syndrome with missense mutation in *COL3A1*. Am J Respir Crit Care Med 197:661–662
32. Wightman JM, Gladish SL (2001) Explosion and blast injuries. Ann Emerg Med 37:664–678
33. Janssen R, Piscaer I, Franssen FME, Wouters EFM (2019) Emphysema: looking beyond alpha-1 antitrypsin deficiency. Expert Rev Respir Med 13:381–397
34. Kim EJ, Elicker BM, Maldonado F et al (2010) Usual interstitial pneumonia in rheumatoid arthritis-associated interstitial lung disease. Eur Respir J 35(6):1322–1328
35. Antoniou KM, Margaritopoulos GA, Goh NS et al (2015) Combined pulmonary fibro-sis and emphysema in scleroderma lung disease has a major confounding effect on lung physiology and screening for pulmonary hypertension. Arthritis Rheum 68(4): 1004–1012
36. Packard TA, Li QZ, Cosgrove GP, Bowler RP, Cambier JC (2013) COPD is associated with production of autoantibodies to a broad spectrum of self-antigens, correlative with disease phenotype. Immunol Res 55(1):48–57

Affiliations

Samia Boussouar[1] · Amira Benattia[2] · Jean.-Baptiste Escudié[3] · Laure Gibault[4] · Frédérique Capron[5] · Anne Legrand[6] · Pierre-Yves Brillet[7] · Xavier Jeunemaitre[6,8] · Philippe A. Grenier[9] · Elie Mousseaux[8,10] · Michael Frank[6,8] · Olivier Sanchez[11]

1 Imagerie Cardiovasculaire et Thoracique (ICT), Hôpital Pitié-Salpêtrière, Assistance Publique-Hôpitaux de Paris, Paris, France, ICT Cardiovascular and Thoracic Imaging Unit, LIB Biomedical Imaging Laboratory INSERM, CNRS, ICAN Institute of Cardiometabolism and Nutrition, Sorbonne Université, Pitié-Salpêtrière Hospital (AP-HP), 47-83 Boulevard de l'hôpital, 75651 Paris CEDEX 13, France

2 Service de Pneumologie, Hôpital Saint Louis, APHP, Paris, France

3 Pôle Informatique Médicale et Santé Publique, Hôpital Avicenne, APHP, Paris, France

4 Université Paris Descartes - Service d'Anatomie Pathologique- Hôpital Européen Georges Pompidou – AP-HP, Paris, France

5 Sorbonne université - Service d'anatomie pathologique- Hôpital Pitié-Salpêtrière-Ch. Foix– AP-HP, Paris, France

6 Université de Paris Centre de Référence des Maladies Vasculaires Rares et service de génétique, HEGP, AP-HP et Inserm U 970, Paris, France

7 Université Paris 13, Sorbonne Paris Cité, EA2363 'hypoxie et poumon', Paris- Service de Radiologie- Hôpital Avicenne- AP-HP-, Bobigny, France

8 Université de Paris Centre de Référence des Maladies Vasculaires Rares et service de génétique, VASCERN MSA European Reference Centre, HEGP, AP-HP et Inserm U 970, Paris, France

9 Département de Recherche Clinique et Innovation, Hôpital Foch, Suresnes, France

10 Université de Paris, Service d'Imagerie Médicale, Hôpital Européen Georges-Pompidou, APHP, Paris Centre de Recherche Cardiovasculaire (PARCC), Paris, France

11 Université de Paris - Service de Pneumologie et Soins Intensifs, Centre de Compétences Maladies Rares Pulmonaires - Hôpital Européen Georges Pompidou – AP-HP – INSERM UMRS 1140, Paris, France